

HEATABLE OPTICAL ANALYZE SYSTEM FOR HIGH TEMPERATURE ABSORBERS

Bernhard Hoffschmidt¹, Markus Sauerborn¹, Max Wagner¹ and Rainer Telle²

¹ Solar-Institut Juelich at the University of Applied Sciences Aachen, D-52428 Juelich, Germany

² Institute of Mineral Engineering, RWTH Aachen, D-52064 Aachen, Germany

1. Abstract

Solar thermal power plants concentrate sunlight onto special absorbers that convert the radiation into thermal energy. The used ceramic absorbers in the solar tower power plant of Juelich are designed for thermal stability and high absorption. The surface properties should be optimized in different ways to increase the efficiency further. A new setup allows measurements of different optical and thermal quantities. The ceramic absorber cups can be heated in an oven element more than 800 °C, the front surface remains freely accessible for optical measurements. So the absorption and reflection as a function of temperature can be determined. For reflection measurements, the absorber is illuminated with a parallel source of radiation from a range of directions. With an integrated spectrometer connected to a measuring collimating lens the spectral reflectance is determined from different view angles. The spectral radiation factor $\beta(\lambda)$ is determined by comparing the reflection of a white standard with the reflection of the test surface.

2. Introduction

Concentrating Solar Power Plants (CSP) use direct sunlight and concentrate it with mirrors on an absorber that heats a fluid like air, water or molten salt [1]. The water is either directly converted into steam or indirectly using a heat exchanger. A steam turbine and a generator are used to produce electrical energy.

The solar tower plant in Juelich is a large scale test facility that started operation in 2008. It uses an open volumetric receiver, which is composed of small porous ceramic modules (about 0.02 m² each). These modules are made of silicon-infiltrated silicon carbide (SiSiC). The radiation of the heliostat field is concentrated on the absorber elements. These can reach temperatures up to 1000 °C and heat up air to the working temperature of 680 °C [1], a temperature that could not be reached with water or molten salt.

In order to develop more efficient absorber elements, their optical properties must be known. At the Solar-Institut Juelich (SIJ) a setup has been developed, which is able to determine the angular distribution of the spectral reflection and absorption of absorber surfaces at different temperatures, a heatable optical spectral analysis goniometer (HOSAG). The construction and function of the measurement system is described in section 4.

Some sample materials that are used for measuring solar radiation or can be found in other solar applications are analyzed. The radiance factor of zirconium oxide at different temperatures is been quantified. Furthermore the hemispheric reflection and emission at room temperature can be determined. The spectrum of Aluminum oxide as a high temperature resistant reflector gives an impression of its reflection behavior at different wavelengths. For all sample materials there are microscope images which help to understand the optical behavior of the surfaces.

3. Basics

3.1 Black body radiator

A black body radiator is a body which absorbs all incoming radiation and emits the maximum possible energy according to its temperature. So the values for absorbance and emittance are 1. The radiant exitance is dependent on the wavelength. Planck's Law gives the equation for a black body radiator at a temperature T .

$$M_{\lambda} = \frac{2\pi hc^2}{\lambda^5} \frac{1}{e^{\frac{hc}{\lambda kT}} - 1} \quad (\text{eq. 1})$$

For higher temperatures the curve gets to lower wavelengths. The sun has got a effective surface temperature of 5778 K and emits radiation from about 250 nm until 2500 nm. The maximum of the curve lies at 500 nm. Integrated over all wavelengths the radiant exitance gets to $M = \sigma T^4$. A body at room temperature emits the maximum at about 10 μm .

3.2 Absorption, reflection and transmission

Radiation that is impacting on matter can be absorbed, reflected or transmitted. The according quantities are the absorbance α , reflectance ρ and transmittance τ . With the incident radiation flux Φ_i the radiation balance can be written as

$$\alpha + \rho + \tau = 1 \quad \text{with} \quad \alpha = \frac{\Phi_a}{\Phi_i}, \quad \rho = \frac{\Phi_r}{\Phi_i} \quad \text{and} \quad \tau = \frac{\Phi_t}{\Phi_i}. \quad (\text{eq. 2-5})$$

For opaque materials ($\tau=0$) the equation reduces to $\alpha + \rho = 1$. One conclusion of this formula is that highly reflecting materials are bad absorbers.

3.3 Radiance factor

The radiance L with the unit $\text{W m}^{-2} \text{sr}^{-1}$ is defined as the flux per unit solid angle and projected area. For the measurement system another term is useful: The spectral radiance factor β is the ratio of a surface's radiance L_S and the radiance L_D of a perfect diffusely reflecting standard. With a spectrometer all terms can be measured as a function of wavelength.

$$\beta(\lambda) = \frac{L_S(\lambda)}{L_D(\lambda)} \quad (\text{eq. 6})$$

4. Experimental setup

4.1 Mechanics

The major components of the test setup are arranged inside a light-tight box which prevents disturbing influences by ambient lighting. The absorber element is placed on a bracket in a cylindrical radiation heater. The heater is secured with a surrounding insulation in a tube, thus forming a rotary furnace. In figure 1 the cover is demounted for a better overview. An angle positioner on the bottom plate moves the oven around a vertical axis of rotation. The angle transmitter at the upper end of the axis measures the surface's angle to the incident radiation. A rotation about a longitudinal axis is also possible with a special design. Parallel light from the radiation source falls through a circular opening in the wall of the box directly on the front side of the absorber element. The reflected radiation passes through a collimating lens into an optical fiber of a spectrometer. Moved by a step motor, a pivoting measuring arm drives the probe to the required measuring angles.

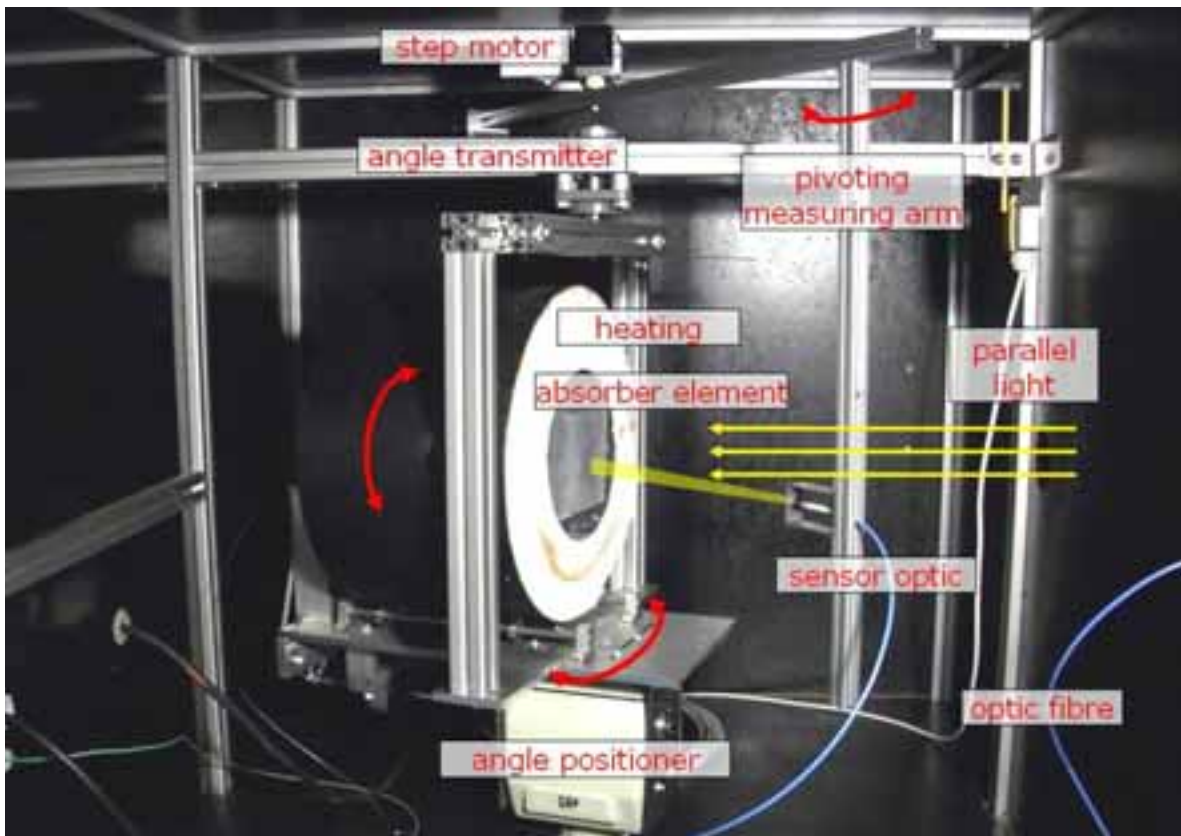


Fig. 1: Setup of the measurement system

4.2 Parallel Light Source

The parallel light source uses a white light emitting diode which simulates the sun's radiation. The spectrum of the LED is shown in figure 2. The first importance is the parallelism of the light and the continuous distribution of wavelengths. The mirror is coated with a metal on the outside. So the light does not have to pass through a glass plate. The reflection is higher and more precise. Because of the polished parabolic form the focus is very precise. A light source which is placed in the focus is reflected as a parallel beam.

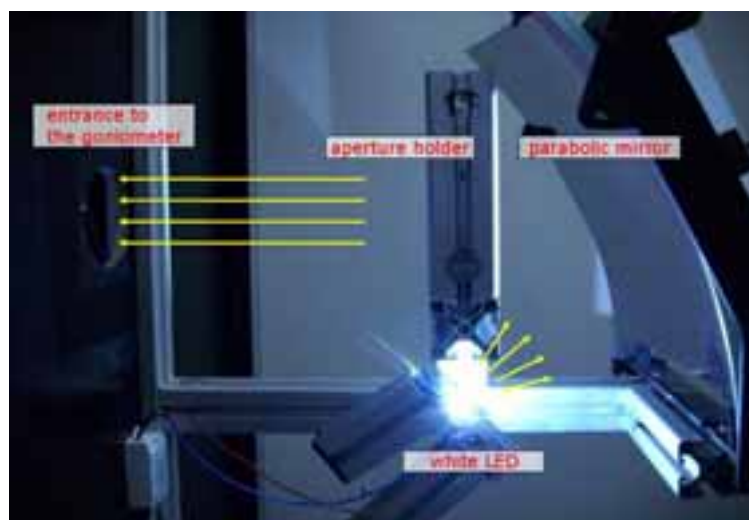


Fig. 2: Parabolic mirror and light emitting diode in the focus

4.3 Geometry and angles

The parallel light arrives into the box on a fixed axis. All angles are defined with respect to this axis. The measuring surface can be rotated by an angle ϑ_a . The sensor's position is defined by the angle ϑ_s . So the difference between these two angles gives an angle ϑ that describes the orientation of the sensor to the surface normal. For $\vartheta_s < \vartheta_a$ the angle ϑ has a negative value. The absorber element can also be turned around its longitudinal axis with the angle φ , so that all directions of incoming radiation can be simulated.

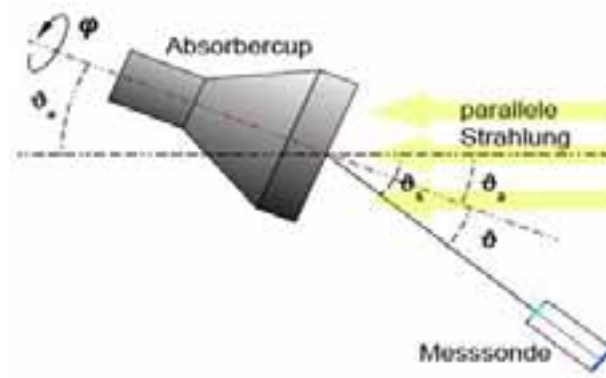


Fig. 3: Definition of the measuring angles

4.4 White standard

The white standard is a disk of PTFE (polytetrafluoroethylene). It has a reflectance of 96 % and is nearly constant for all wavelengths which are relevant for the measurement. It has Lambertian characteristics and is used for both measurements of the direct and hemispherical reflection.

5. Sample Materials

5.1 Silicon infiltrated silicon carbide

Figure 4 shows a plate of silicon infiltrated silicon carbide (SiSiC) and a picture of the plate made by a reflected light microscope. Because of the different orientation of the crystal planes the light is reflected into various directions.

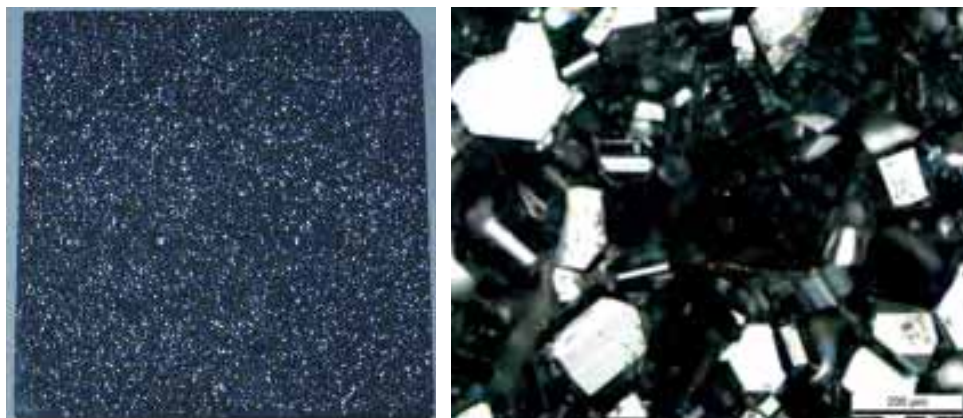


Fig. 4: Plane plate of SiSiC ceramic test material in two different scaled views

5.2 Zirconium oxide

The second sample material is zirconium oxide (ZrO_2), stabilized with calcium. The right part of figure 5 shows an image made by an electron microscope. It is a porous structure with a glazed surface. The gray and black regions are the pore spaces.

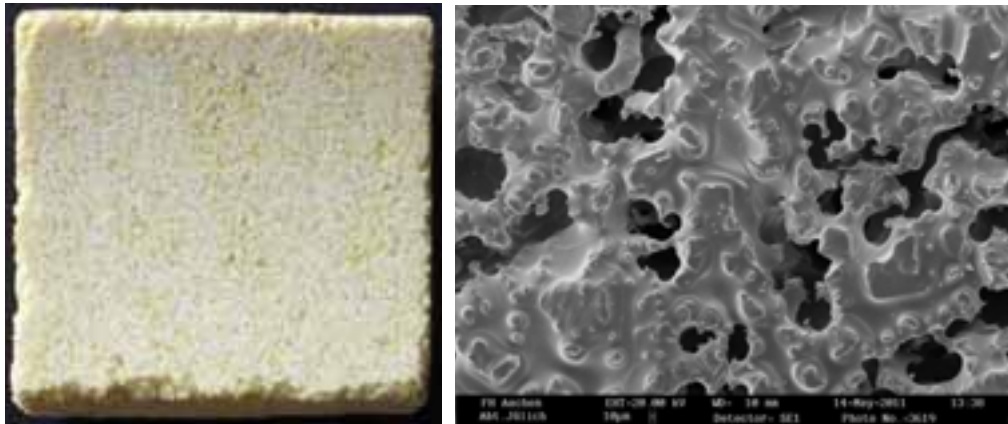


Fig. 5: Plane plate of zirconium oxide ceramic test material in two different scaled views

5.3 Aluminium oxide

Figure 6 shows a plane plate of aluminium oxide (Al_2O_3) in the original size. Because of its high temperature-resistance and good reflectance in the visible and near infrared region (figure 11) it is used as a reflector for radiation with a high flux density. The surface of the material is very plane, the grains of the microstructure are close to each other.

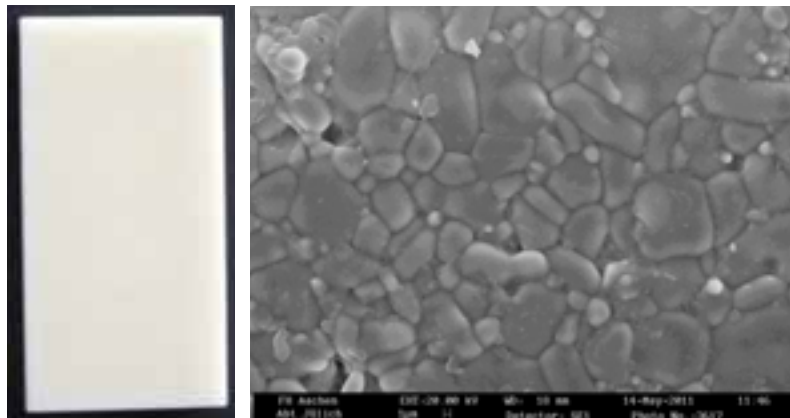


Fig. 6: Plane plate of aluminum oxide ceramic test material in two different scaled views

6. Results

6.1 Spectral radiance factor

The first diagram of figure 7 shows the radiance factor as a function of wavelength. The curves are plotted in a different color according to their measurement angles, which are presented in the legend. In the diagram below the mean radiance factor is plotted against the angle θ .

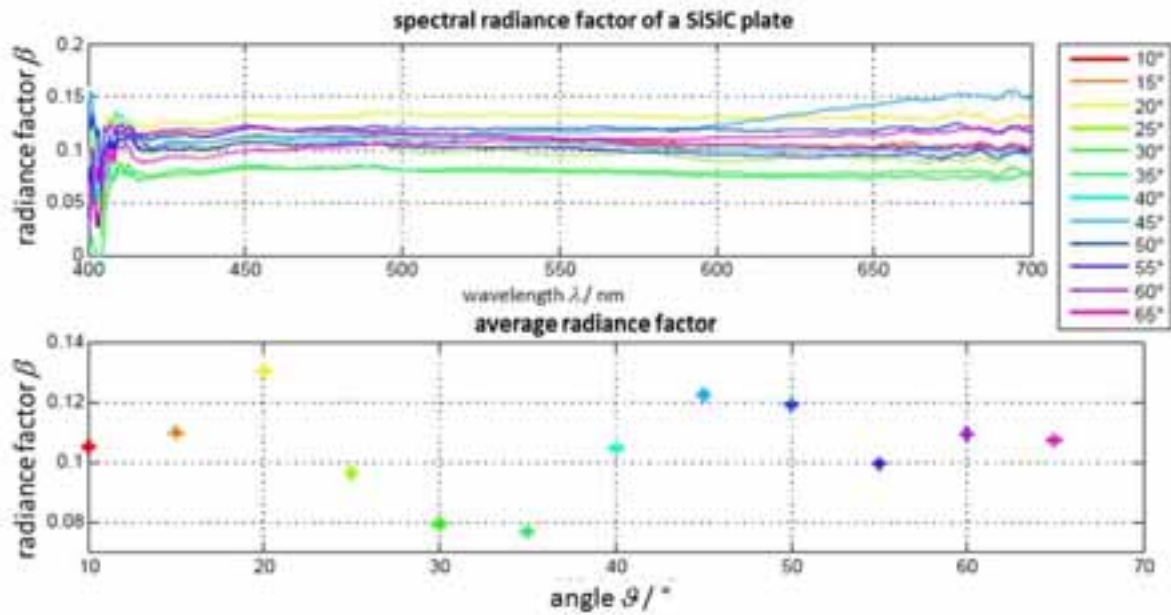


Fig. 7: Spectral radiance factor at different viewing angles of a sample plate of SiSiC

The radiance factor is almost independent of wavelength. That means that the sample's material is a gray reflector. The radiance factor is changing with the viewing angle. There is no apparent trend because the material structure is not homogeneous in the measurement area.

6.2 Measurements at high temperature

Figure 8 shows three signals. The green line is the reflection of the light of the parallel light source. It is the typical shape of a white emitting diode. Because of its temperature of 600 °C the sample emits radiation with wavelengths starting at about 600 nm, the surface glows with a red color. This emission is represented by the red curve. The infrared fraction is a lot higher than the visible one, the curve is increasing very quickly into the infrared region. Both signals, the reflection and emission are detected by the optical sensor. The blue curve shows the overlap of the light reflection and thermal emission.

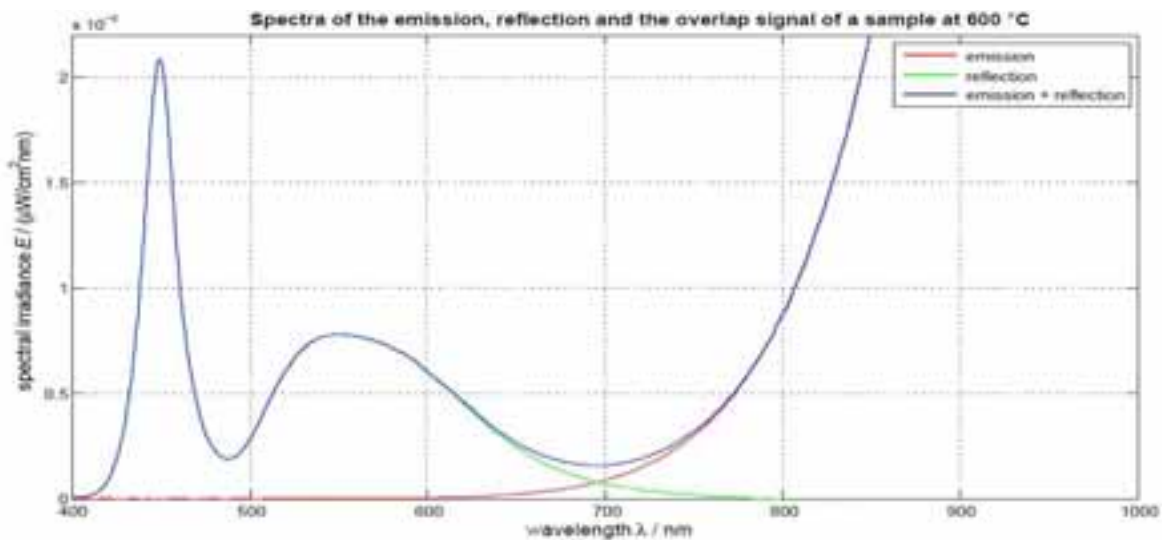


Fig. 8: Spectra of the emission, reflection and the overlap signal (porous geometry of SiSiC)

The surface of the zirconium oxide is measured at different temperatures. The angle of the incident radiation

ϑ_a is 20° , the sensor is placed at a position with the angle ϑ_s of 40° . As follows, the measuring angle ϑ is 20° to the surface's normal.

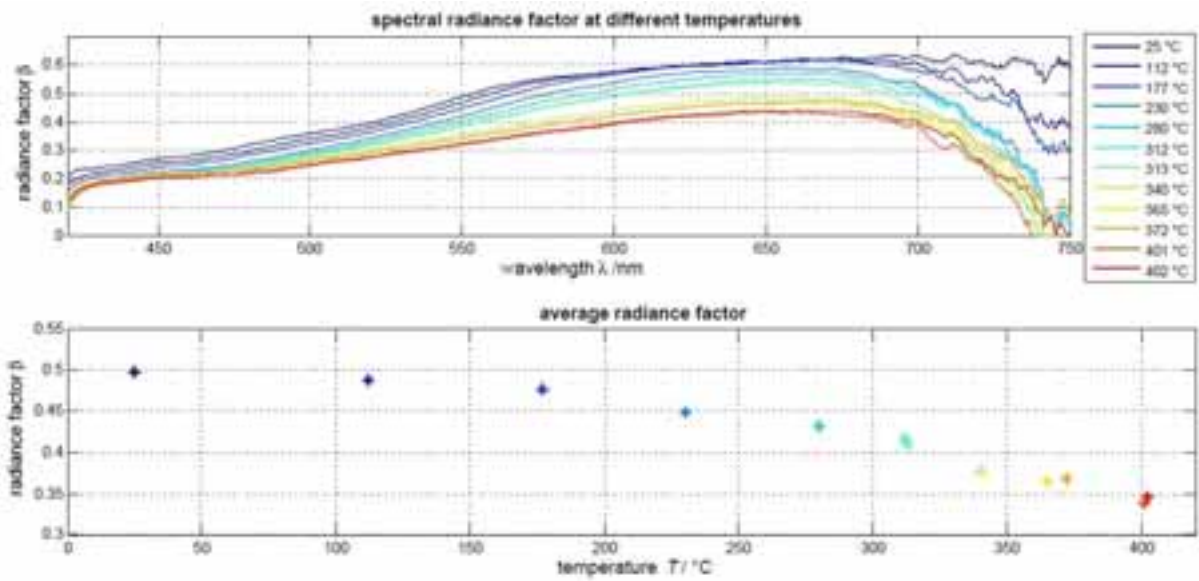


Fig. 9: Spectral radiance factor at different temperatures of a sample plate of zirconium oxide

The curves of the radiance factor are different for every temperature. The shapes of them are similar, described for a temperature of 400°C . The factor starts from 0.1 at 420 nm until 0.55 at 660 nm. After this maximum it decreases quickly to zero at 740 nm.

The averaged radiance factor is getting lower for higher temperatures. At room temperature the factor at room temperature is 0.5 and 0.35 at 400°C . Because of the method of the temperature measurement the accuracy of the factor has a range. That is why the points at 401°C and 402°C differ in 0.01.

6.4 Hemispherical measurements

The hemispherical measurements are made with a system that determines the hemispherical spectral reflection of a surface. Additionally the absorption of solar radiation is calculated. It is 89.1 % for the sample plate of SiSiC.

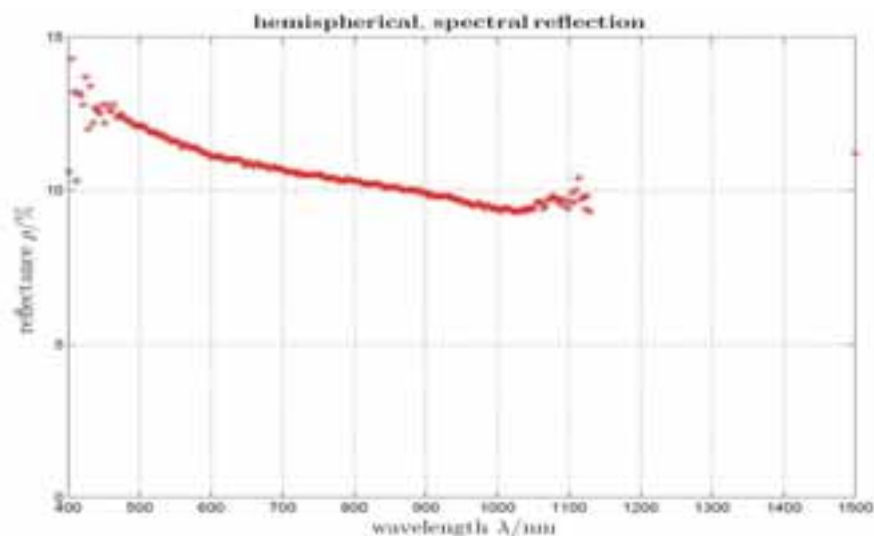


Fig. 10: Spectral radiance factor at different viewing angles of a sample plate of SiSiC

The hemispheric spectral reflection of the plate is decreasing from 400 nm until 1020 nm, the minimum in the reflectance. So the absorption of radiation is the highest at this wavelength around 1020 nm. From there the reflection increases again. Between 1200 nm and 1900 nm there are no spectrally resolved data but a median. The maximum of the respective weighting function lies at 1500 nm. The reflectance in this NIR region is comparable with values around 500 nm.

Figure 11 shows measurements of the hemispherical spectral reflection of aluminum oxide. They are made at three different points on the sample surface.

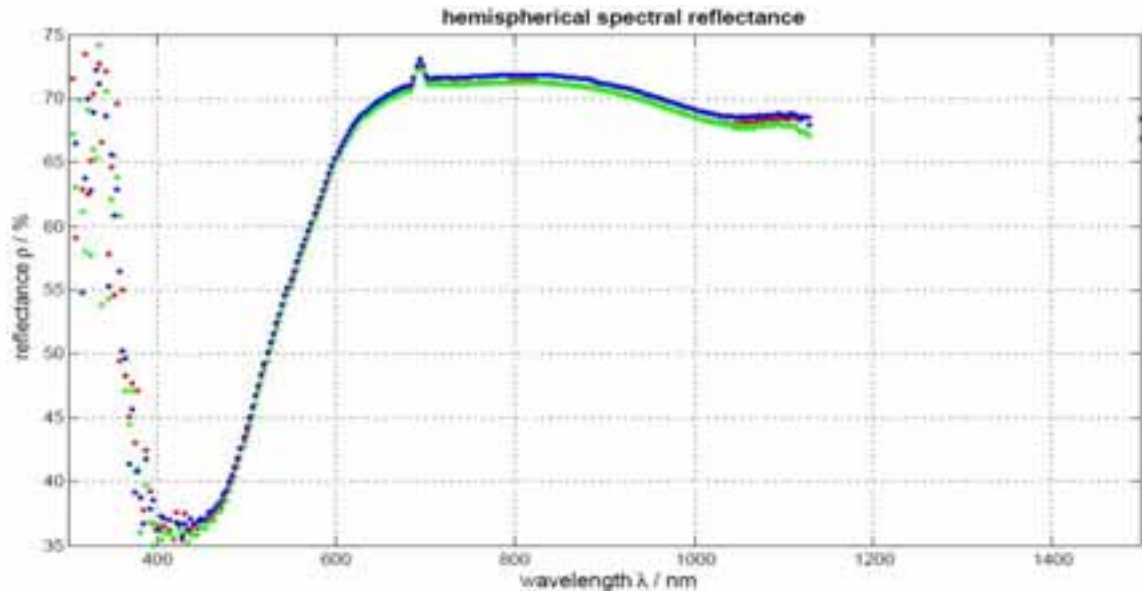


Fig. 11: Hemispherical spectral radiance factor of a sample plate of aluminum oxide

From the minimum of 35 % at 400 nm the reflectance increases quickly to over 70 % at 650 nm. The curve runs at a level of 70 % \pm 2.5 % from 650 to 1500 nm. That is why it can be used as a good reflector for solar like radiation. Besides the region until 600 nm, the visible and near infrared range is usable for a high and stable reflection.

6.5 Hemispherical emission

The emission measurement is made with a system which uses an integrating sphere coated with a diffuse gold. Its detector is sensitive for wavelengths in the range from 8 to 14 μ m. So the emittance is determined by integrating over this interval. The plate of aluminium oxide is been measured at several points on the surface at room temperature. The median of the emittance is $\epsilon = 88.4$ with a standard deviation of 1.8.

7. Conclusion and further steps

A measurement system was developed which is able to determine the angle-dependent spectral reflection of surfaces at different temperatures. The heatable optical spectral analyze goniometer (HOSAG) fulfills all the requirements.

The determination of the angle-dependent spectral radiance factor provides information about the reflection properties of a testing sample. The measuring surface can be heated up to stable temperatures about 1000 °C. Furthermore the angle-dependent emission of a heated body can be measured.

Further developments will comprise the automatization of the data recording and a computerized control of the angular adjustments. The wavelength range of the spectrometer is restricted to 250-1100 nm. With another or an additional spectrometer values for the near infrared region could be analyzed.

Acknowledgements

The project was supported by the German Ministry of Education and Research under contract no. 1727X08

References

- [1] B. Hoffschmidt, V. Vernandez, A.G. Konstandopoulos, Development of Ceramic Volumetric Receiver Technology, Forschungsbericht: DLR FB. - 10(2001). - pages: 51-61.
- [2] Physikalisch-Technische Bundesanstalt <http://www.ptb.de/cms/fachabteilungen/abt4/fb-45/ag-452/begriffe.html> 2011/03
- [3] A. Höpe, K.-O. Hauer, Three-dimensional appearance characterization of diffuse standard reflection materials, Physikalisch-Technische Bundesanstalt, Metrologia 47, 2010, pages 295-304
- [4] Michael Foos, Solar Simulators, product information of LOT group Europe, Im Tiefen See 58, 64293 Darmstadt, 2010
- [5] W. Erb and M. Krystek, Reflection behaviour of the perfect reflecting diffuser under real conditions, Physikalisch-Technische Bundesanstalt (PTB), Optik 69 No.2